

Finite-size correlation behavior near a critical point: a simple metric for monitoring the state of a neural network

Eyisto Aguilar Trejo^{1,2}, Daniel A. Martin^{1,2}, Tomas S. Grigera^{2,3,4,5}, Sergio A. Cannas,^{2,6} Dante R. Chialvo^{1,2}

¹ *Instituto de Ciencias Físicas (ICIFI-CONICET),*

Center for Complex Systems and Brain Sciences (CEMSC3),

*Escuela de Ciencia y Tecnología, Universidad Nacional de Gral. San Martín,
Campus Miguelete, 25 de Mayo y Francia, 1650, San Martín, Buenos Aires, Argentina*

² *Consejo Nacional de Investigaciones Científicas y Técnicas (CONICET),*

Godoy Cruz 2290, 1425, Buenos Aires, Argentina

³ *Instituto de Física de Líquidos y Sistemas Biológicos (IFLySiB-CONICET)*

Universidad Nacional de La Plata, 1900, La Plata, Buenos Aires, Argentina

⁴ *Departamento de Física, Facultad de Ciencias Exactas,*

Universidad Nacional de La Plata, 1900, La Plata, Buenos Aires, Argentina

⁵ *Istituto dei Sistemi Complessi, Consiglio Nazionale delle Ricerche, via dei Taurini 19, 00185 Rome, Italy and*

⁶ *Instituto de Física Enrique Gaviola (IFEG-CONICET),*

Facultad de Matemática Astronomía Física y Computación,

Universidad Nacional de Córdoba, 5000, Córdoba, Argentina.

In this note, a correlation metric κ_c is proposed which is based on the universal behavior of the linear/logarithmic growth of the correlation length near/far the critical point of a continuous phase transition. The problem is studied on a previously described neuronal network model for which is known the scaling of the correlation length with the size of the observation region. It is verified that the κ_c metric is maximized for the conditions at which a power law distribution of neuronal avalanches sizes is observed, thus characterizing well the critical state of the network. Potential applications and limitations for its use with currently available optical imaging techniques are discussed.

The study of critical phenomena in the brain [1–3] benefited from different experimental approaches. The most common by far is the statistical characterization of the so-called neuronal avalanches, consisting of sudden increases in the activity which exhibits power-law distribution of sizes and durations [4]. This analysis has been reproduced over different setups (i.e., tissues and experimental conditions, see e.g. [5, 6]), and in a diversity of numerical simulations. Several caveats, such as subsampling [7], thresholding [8], or the artifacts introduced by the coexistence of overlapping avalanches [9], as well as alternative interpretations of the results [10] prompted the exploration of complementary approaches.

One of them, which can be considered as the signature of a continuous phase transition, is the behavior of the correlation length ξ , which diverges with the size of the system (see e.g. [11]), a fact that was shown to be exhibited by the large scale brain dynamics [12, 13]. More recently the same divergence of ξ was demonstrated in small areas of the behaving mice brain [14]. This measures were facilitated by the use of novel opto-genetic techniques [15], which allows for the recording of the individual activity of a relatively large number of neurons. In that work, a proxy of the standard finite size analysis, named Box-Scaling (B-S) was used, [16] in which the observation window, instead of the system size, is varied. An estimate of the correlation length ξ was found to grow linearly or logarithmically with window size depending if the system is near or far from the critical state, respectively. Based on this previous results, the purpose of this

letter is to introduce a simple metric, describing the typical finite-size behavior of the correlation length near criticality to distinguish critical from non-critical dynamics. To this end, we study a simple model of neuronal dynamics that can be tuned towards and away from the critical point of a second-order phase transition dynamics, as the control parameter is varied. For completeness, we contrast the new metric with the most common analysis, the avalanche size distribution statistics.

The paper is organized as follows: Next we describe the model and define the observables, first for the standard metric of avalanches analysis and then for the finite-size correlation based metric. After that, the main results are described by contrasting both metrics. The paper close with a short discussion of the limitations and potential applications.

Model and observables- Briefly, the model studied is an excitable cellular automata on a square lattice of interconnected neurons under periodic boundary conditions plus a certain degree of quenched disorder. Each neuron activity is described by the Greenberg & Hastings' excitable three states dynamics [17]. There is a single control parameter T that determine the threshold for being excited by other neurons. The results rely on universal behavior of the correlation function in critical phenomena, thus they are model independent. Because of that we skip for now further details of the model, which can be consulted if needed in the Appendix.

We run simulations for several values of the control parameter T which previous results [16] indicate produces

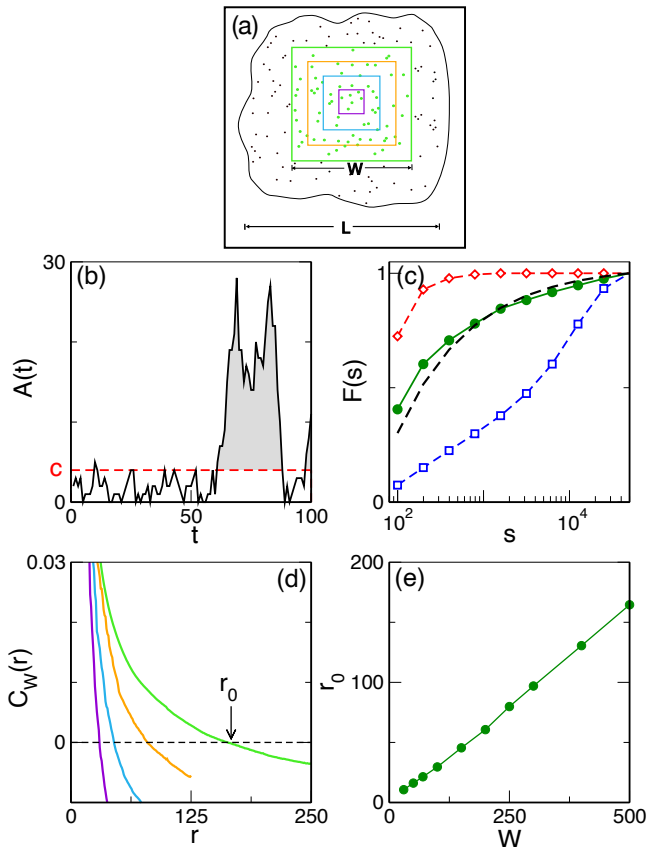


FIG. 1. System scheme. (a) A system of characteristic size L is studied through boxes of side W . Only neurons inside the box are recorded. (b) Example of the time series A , the total number of neurons active inside a window, as a function of time. An avalanche, (filled with gray), is defined as the total activity above a threshold c , computed from the time at which A becomes greater than c to the next time that it becomes lower than c . Panel (c) shows the cumulative avalanche size distribution function $F(s)$ as a function of avalanche size s , for three different situations: subcritical ($T = 0.33$, open blue squares), supercritical ($T = 0.31$, open red diamonds) and close to criticality ($T = 0.318$ green filled circles). The dashed line represents the theoretical expectation for the avalanche size distribution expected at criticality. (d) The connected correlation function of a window of size W , $C_W(r)$, for several values of W , computed at criticality. From left to right, $W = 50$ (violet line), $W = 150$ (cyan), $W = 250$ (orange), $W = 500$ (light green). The characteristic length r_0 for $W = 500$ is marked with an arrow, as an example. (e) Characteristic length r_0 as a function of window size W at the critical state. Results computed on a system of size $L = 1000$, $k = 24$, $\pi = 0.01$ and $T = 0.318$. In panels (b) and (c), window size $W = 500$ was used.

subcritical (for very high values of T), supercritical (for very low values of T) or critical dynamics. To accumulate enough statistics, we run 20 numerical simulations (lasting 10^5 time steps, discarding the initial 5000 time steps). For each simulation we constructed a network with the same average parameters k and π (i.e., they are

stochastic realizations). To mimic experimentally relevant situations, we record the dynamics of the neurons within a square window of $W \times W$ neurons (with $W \leq L$), see Fig. 1-a.

Metric based on the avalanche's size distribution- The standard procedure for avalanche analysis [4] focuses in the estimation of the distribution of avalanche size and duration. For that, the total activity of the neurons inside a given (spatial) window is computed as a function of time, $A(t) = \sum_{i \in W \times W} \delta_{S_i(t), 1}$ ($S_i(t) = 1$ if neuron i is spiking at time t). Notice that in the standard procedure it is usual to group the activity on time bins approximately equal to the average of one inter-spike-interval. The coarse grain scale of the model considered here (i.e., only three discrete states) determines that we must compute $A(t)$ for each time unit, as mentioned above. Also, since for the conditions of our case $A(t)$ very rarely becomes zero, following [8], we need to define a non-zero avalanche threshold c . Avalanche size is defined then as the total activity above c between two consecutive zeros of $A(t) - c$, see Fig. 1-b. At criticality, avalanche size distribution, $P(s)$, where (s is the avalanche size), is expected to have a power law distribution, $P(s) \propto s^{-\tau}$, where, in the mean field directed percolation universality class, $\tau = 3/2$ [4, 18]. The value of c is chosen to maximize the number of avalanches for each value of T and W .

The goodness of fit to a power of the neuronal avalanches size distribution has been considered as suggestive for critical dynamic, which taken in isolation may call for caveats, precautions and criticisms [19]. Nonetheless, when used in conjunction with other measures it can overcome some of its limitations [10]. In that regards, Shew et al. [20] defined, from the cumulative avalanche size distribution, $F(s)$, a metric κ_S , which is [20]:

$$\kappa_S = 1 + \frac{1}{m} \sum_{k=1}^m F^{NA}(\beta_k) - F(\beta_k) \quad (1)$$

Where $F^{NA}(\beta) = \frac{1 - (s_{min}/\beta)^{\tau-1}}{1 - (s_{min}/s_{max})^{\tau-1}}$, is the theoretical distribution for the critical case, and β_k are m power-law distributed values ranging from $s_{min} = 50$ to $s_{max} = 50000$. We have used $m = 10$ as in [20]. For avalanche size distributions with exponent τ $\kappa_S = 1$, while $\kappa_S \geq 1$ for super/subcritical situations. We have computed κ_S assuming $\tau = 3/2$.

Metric based on finite-size scaling of correlations- Following previous work [16], we computed the connected correlation function on a window of size W , as the correlation of the fluctuations of the neuronal activity, with respect to its *instantaneous spatial average* [12–14, 16, 21–25]:

$$C_W(r) = \frac{1}{c_0} \frac{\sum_{i,j} \delta v_i \delta v_j \delta(r - r_{ij})}{\sum_{i,j} \delta(r - r_{ij})} \quad (2)$$

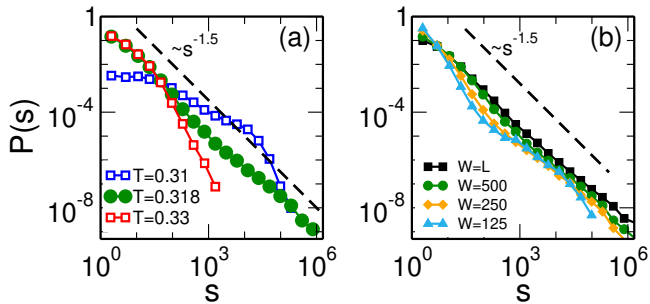


FIG. 2. Avalanche size distribution computed on a window of size $W = 500$, for different values of T in (a) and for $T = 0.3180 \simeq T_C$ and several values of W in (b). The dashed lines, in both panels, show a power law with exponent $-3/2$ as a guide to the eye. All parameters as in Fig. 1.

where $\delta(r - r_{ij})$ is a smoothed Dirac δ function selecting pairs of neuron states at a distance r (in practice, we have computed $C_W(r)$ for integer values of r , averaging all points at distances $(r - 0.5, r + 0.5]$); r_{ij} is the Euclidean distance from the site i to site j ; δv_i is the value of the signal v_i of site i at time t , after subtracting the the *instantaneous spatial average* of signals $V(t) = (1/N) \sum_i^N v_i(t)$, i.e., $\delta v_i(t) = v_i(t) - V(t)$; and $\frac{1}{c_0}$ is a normalization factor to ensure that $C_W(r = 0) = 1$. We consider that $v_i = 1$ if neuron i is in the active ($S_i = 1$) or refractory ($S_i = 2$) state and $v_i = 0$ otherwise. We compute Eq. 2 once every 20 time steps (i.e., we take information for 4750 time steps for each network), and then average the result over different time steps and different networks. An estimate of the correlation length can be calculated from Eq. 2 as r_0 , the first zero crossing of the function (i.e., $C_W(r_0) = 0$). We stress that the implementation of r_0 considers averages of *instantaneous* correlations computed inside a window.

We measure $C_W(r)$ for several values of W , ranging from W_{min} to W_{max} . For equilibrium thermodynamic systems, the behavior of r_0 as a function of W , for fixed L , is known in the limiting cases: $r_0 \propto W$ for $W \ll L \ll \xi$ at criticality, while $r_0 \propto \xi \log(W/\xi)$ for $\xi \ll W_{min}$, where ξ is the standard correlation length, see [16, 24].

To estimate the distance to criticality, for each explored window size W , we propose a linear relation among r_0 and W , $r_0(W) = a_W \times W$, and also, a logarithmic growth $r_0(W) = r_0(W_{min}) + b_W \log(W/W_{min})$. Similar to Eq. 1, we define

$$\kappa_C = \frac{CV_s^2}{CV_c^2 + CV_s^2}, \quad (3)$$

where CV_s is the coefficient of variation of $\{b_W\}$ and CV_c is the coefficient of variation of $\{a_W\}$. Notice that $0 \leq \kappa_C \leq 1$, where $\kappa_C = 0$ is for a perfect logarithmic growth and $\kappa_C = 1$ is for perfect linear growth. The definition of (3) is insensitive to a change in the spatial scale ($r \rightarrow \lambda r$). More sophisticated measures can also be

proposed.

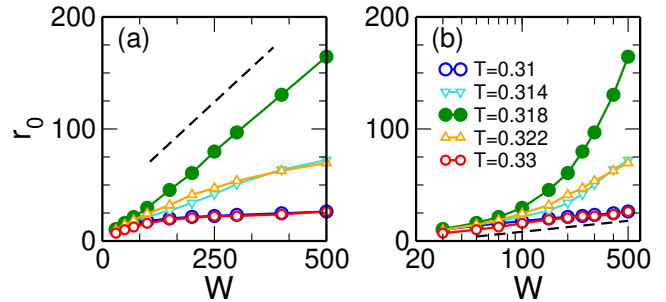


FIG. 3. Characteristic correlation length as a function of window size W obtained at various control parameter values T (indicated in the legend). The same results are plotted in linear scale in panel (a) and in linear-logarithmic scale in panel (b). All other parameters as in Fig. 1.

Results- As a reference, we first characterize the behavior of the avalanche size distribution, computed inside of a window of size $W = 500$, for different values of T . The results are shown in Fig. 2-a. In the subcritical state ($T = 0.33$), activity is low, and there are no large avalanches, for any value of c . In the supercritical case ($T = 0.31$), activity is very high, being always larger than zero. The avalanche size distribution has a hump for $s \sim 10^5$. Hump position depends on c , showing system-wide avalanches (i.e., dragon kings) for low c . In the critical case ($T \simeq 0.318$), avalanche size distribution follows closely a power law with exponent $\tau = 3/2$. The best collapse exponent depends on c , and values compatible with τ in the range 1.3-1.7 can be obtained. For the critical data in the figure, it can be seen that for small values of s (i.e., $s < 100$), there is an excess of avalanches, compared to the expected. This excess is a consequence of subsampling, and is not present for $W = L$, while it is even larger for small values of W , such as $W = 125$, see Fig. 2- b. This difference may be due to the contributions of avalanches that enter or leave the window from the rest of the system, as already discussed in the context of avalanches in the qKPZ model, see Ref. [26].

Next, we turn to describe the correlation behavior on the same data used to study avalanches. The characteristic correlation length r_0 as a function of window size W , for $W_{min} = 30$, $W_{max} = 500$, is shown in Fig. 3. For the critical value of the threshold ($T = 0.318$), there is a linear relation among r_0 and W , while for sub and supercritical regimes, r_0 is smaller, and the growth of r_0 with W is logarithmic. Slightly subcritical and supercritical cases, (plotted with triangles), show intermediate results. Similar results can be found when $C_W(r)$, Eq. 2, is computed for the whole system ($W = L$), varying system size, as shown in [16] for the Ising paramagnetic-ferromagnetic model and for a different neuronal model [7].

The values of κ_S and κ_C , extracted from avalanche size

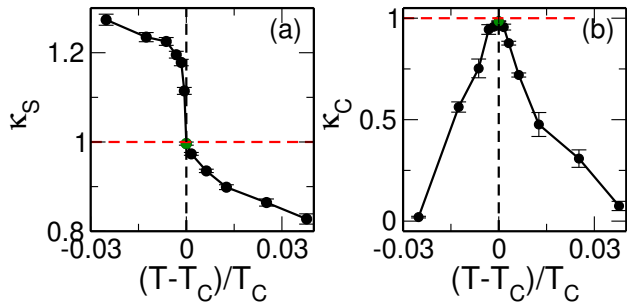


FIG. 4. Behavior of the two metrics as a function of T near the critical point of the neural model: κ_S in panel (a) and κ_C in panel (b). All other parameters as in Fig. 2 and 3.

distribution and correlation length scaling, are shown in Fig. 4. Avalanche analysis (κ_S), assuming $\tau = 3/2$, yields expected results: $\kappa_S > 1$ (< 1) for supercritical (subcritical) regime, while κ_S is closest to 1 for critical regime, $T = 0.318$ (marked with a green dot). For very subcritical values (high T), κ does not keep on decreasing, probably due to having a short range of s values captured by $P(s)$. The analysis of characteristic length collapse, κ_C , shows compatible results, see Fig. 4-b. The logarithmic fit is better than the linear fit (i.e., $\kappa_C > 0.5$) only for $0.314 < T < 0.322$, having its peak at $T = 0.318$, i.e., the same value as in κ_C .

Finally, to compare the precision of κ_S and κ_C , in Fig. 5-b, we show results in a situation where the control parameter T is varied. It can be shown that close to criticality, the error in κ_C is lower than the error in κ_S . More important, it decays $\sim 1/n$ where n is the number of snapshot used.

Discussion- The original experimental setups where avalanches were measured, used microelectrode arrays of ~ 60 detectors, each of which measures the activity of several neurons with very high (i.e., millisecond) temporal resolution. The experimental constraints were suitable for computing neuronal avalanches, where only the evolution of the total activity as a function of time is required, and it is not necessary to know the spatial location of the spiking neurons. To estimate how close the system is to criticality by using this approach, several parameters need to be defined and adjusted, such as the time binning, minimum and maximum values of considered avalanches, and a non-zero threshold for defining avalanches in the cases the activity never ceases (i.e., as in very large number of neurons). Furthermore, additional experimental caveats need to be considered, such as subsampling [7], windowing (i.e., avalanches involving neurons outside of the observation window), or the existence of several simultaneous unrelated avalanches [9].

Novel opto-genetic techniques allow to study the dynamics of a large number (from one hundred a few thousand) of neurons individually, considering, however a lower temporal resolution, typically in the 30-60Hz

range. Performing avalanches analysis on opto-genetic data would be affected by this low temporal resolution, the thresholding and most important, would not profit from the spatial information of the spiking neurons. In contrast, correlation length computation, which is performed from instantaneous snapshots of the system state does not require its temporal evolution. Moreover, box-scaling should not be affected by sub sampling artifacts, since the value of $C_W(r)$ is computed from the activity of pairs of *observed* neurons at a distance r .

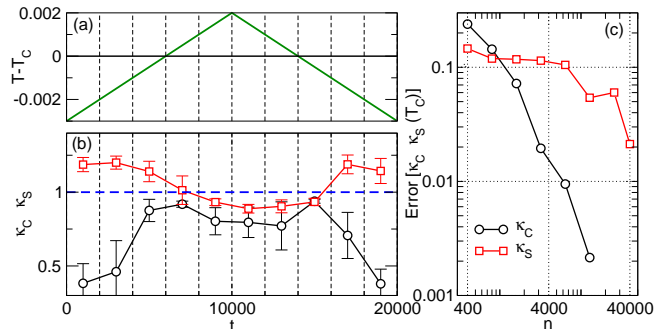


FIG. 5. Behavior of the two metrics for an hypothetical slow change in the network excitability here simulated by changes in the parameter T . Panel (a) shows the temporal evolution of T as a function of time t . Panel (b) shows the estimated mean (\pm SD) κ_S and κ_C , computed over time segments of $n = 2000$ steps. For κ_C , we used spatial windows $W \leq 300$. For κ_S an average of ~ 95 avalanches (range 14-280) were detected in each run and each time window. Panel (c) shows the errors of both estimators computed as the average distance from the measured value and the *real* value, $\kappa_{S/C}^*$ (computed using all time points), as a function of the number of used time points n , at $T = 0.3180 \simeq T_C$. Four simulations were used in each panel. For avalanche analysis, since now n is variable, we have taken s_{min} as 10 times the minimum observed avalanche size, and s_{max} as 0.1 of the largest observed avalanche size.

Overall, the results show that the value of the control parameter T_c (i.e., for critical behavior) inferred via avalanche-size distribution is very close to the value that maximizes the correlation length. Thus, while state of the system can be monitored from either method, notice that the computation of the correlation length is less dependent on parameters, such as the ones needed in the avalanche analysis (e.g., such as bin length, threshold, separation of time scales).

In summary, we have introduced a simple metric, κ_C , describing the typical finite-size behavior of the (instantaneous) spatial correlations of neuronal activity. By construction κ_C is able to distinguish critical from non-critical dynamics and compares well with the usual avalanches analysis which estimates the distribution of the space-integrated activity. In a given experimental situation, the observation of large κ_C values indicating long range *spatial* correlations must be consistent with the simultaneous observation of large values for the *tem-*

poral correlations, as shown previously [27]. Results presented here suggest that the correlation length computations using Box-Scaling are well suited as a complement or a substitute of neuronal avalanche analysis as a useful tool for monitoring criticality on diverse experimental conditions.

APPENDIX

We study a cellular automata model previously described [12, 16, 28], which itself is based on the Greenberg and Hastings model [17], on a two dimensional array of $L \times L$ neurons under periodic boundary conditions. Each neuron j has $k = 24$ output connections chosen as follows: the closest k neurons are initially selected, and then, to mimic a small world topology, each of this connections is rewired with probability $\pi = 0.01$ to another, randomly chosen, postsynaptic neuron within the whole system. The weights of the resulting k nonzero connection weights are taken randomly from an exponential distribution $p(W_{ij} = w) \propto \exp(-w\lambda)$ with $\lambda = 12.5$, as in [28]. Here, the connection matrix does not need to be symmetric and network parameters are fixed (i.e., neither the connections nor W_{ij} evolve with time).

Within this model, time is discrete and each neuron i may be in any of the following three states: quiescent ($S_i(t) = 0$), active ($S_i(t) = 1$) or refractory ($S_i(t) = 2$). At time $t + 1$ a quiescent neuron can become active due to an external input with a small probability r_1 (we have used $r_1 = 10^{-5}$), or if the contribution of all active connections at time t is larger than a threshold T ($\sum_j W_{ij} \delta_{S_j(t),1} > T$); an active neuron will become refractory always, and a refractory neuron will become quiescent with probability r_2 (following [28], we have used $r_2 = 0.3$ throughout the text).

This work was partially supported by Grant No. 1U19NS107464-01 from NIH BRAIN Initiative (USA) and CONICET (Argentina)

[1] P. Bak, *How nature works: The science of self-organized criticality* (Springer Science, New York, 1996).
 [2] D. R. Chialvo, *Physica A* **340**, 756 (2004).
 [3] D. R. Chialvo, *Nat. Phys.* **6**, 744 (2010).
 [4] J. M. Beggs and D. Plenz, *J. Neurosci.* **23**, 11167 (2003).

[5] T. Petermann, T. C. Thiagarajan, M. A. Lebedev, M. A. L. Nicolelis, D. R. Chialvo and D. Plenz, *Proc. Natl. Acad. Sci. USA* **106**, 15921–15926. (2009).
 [6] N. Friedman, S. Ito, B. A. W. Brinkman, M. Shimono, R. E. Lee DeVille, K. A. Dahmen, J. M. Beggs and T. C. Butler, *Phys. Rev. Lett.* **108**, 208102 (2012).
 [7] T. L. Ribeiro, S. Ribeiro, H. Belchior, F. Caixeta and M. Copelli, *PLoS one* **9**, e94992 (2014).
 [8] P. Villegas, S. di Santo, R. Burioni and M.A. Muñoz, *Phys. Rev. E* **100**, 012133 (2019).
 [9] D. J. Korchinski, J. G. Orlandi, S.-W. Son and J. David- sen, *Phys. Rev. X* **11**, 021059 (2021)
 [10] J. Touboul and A. Destexhe, *Phys. Rev. E* **95**, 012413 (2017).
 [11] J. L. Cardy, (ed.) *Finite-size Scaling* (North Holland, Amsterdam, 1988).
 [12] A. Haimovici, E. Tagliacuzzi, P. Balenzuela and D. R. Chialvo, *Phys. Rev. Lett.* **110**, 178101 (2013).
 [13] D. Fraiman and D. Chialvo, *Front. Physiol.* **3**, 307 (2012).
 [14] T. L. Ribeiro, S. Yu, D. A. Martin, D. Winkowski, P. Kanold, D. R. Chialvo, and D. Plenz, *bioRxiv*, 12145 (2020).
 [15] V. Emiliani, A.E. Cohen, K. Deisseroth and M. Häusser, *J. Neurosci.* **35**, 13917–13926 (2015).
 [16] D. A. Martin, T. L. Ribeiro, S. A. Cannas, T. S. Grigera, D. Plenz and D. R. Chialvo, *Sci. Rep.* **11**, 15937 (2021).
 [17] J. M. Greenberg and S. Hastings, *SIAM J Appl Math.* **34**, 515 (1978).
 [18] S. Zapperi, K. B. Lauritsen, and H. E. Stanley *Phys. Rev. Lett.* **75**, 4071 (1995).
 [19] A. Deluca and A. Corral, *Acta Geophys.* **61**, 1351–1394 (2013).
 [20] W. L. Shew, H. Yang, T. Petermann, R. Roy and D. Plenz, *J. Neurosci.* **29**, 15595 (2009).
 [21] Q.-Y. Tang, Y.-Y. Zhang, J. Wang, W. Wang and D. R. Chialvo, *Phys. Rev. Lett.* **118**, 088102 (2017).
 [22] Q.-Y. Tang and K. Kaneko, *PLOS Computational Biology* **16**, 1 (2020).
 [23] A. Attanasi, A. Cavagna, L. Del Castello, I. Giardina, S. Melillo, L. Parisi, O. Pohl, B. Rossaro, E. Shen, E. Silvestri, and M. Viale *Phys. Rev. Lett.* **113**, 238102 (2014).
 [24] A. Cavagna, I. Giardina, and T. S. Grigera, *Phys. Rep.* **728**, 1 (2018).
 [25] B. Mariani, G. Nicoletti, M. Bisio, M. Maschietto, S. Vassanelli and S. Suweis, *arXiv:2105.05070* (2021).
 [26] Y.-J. Chen, S. Papanikolaou, J. P. Sethna, S. Zapperi, and G. Durin *Phys. Rev. E* **84**, 061103 (2011).
 [27] D. R. Chialvo, S. A. Cannas, T. S. Grigera, D. A. Martin, D. Plenz. *Sci. Rep.* **10**(1), 1-7 (2020).
 [28] M. Zarepour, J. I. Perotti, O. V. Billoni, D. R. Chialvo and S. A. Cannas, *Phys. Rev. E* **100**, 052138 (2019).